FINITE ELEMENT ANALYSIS OF AN ENDOSCOPE DURING OPHTHALMIC SURGERY

Jarno Mastomäki, Jan Hošek

Ústav přístrojové a řídicí techniky, ČVUT v Praze, Fakulta strojní, Praha

Czech Technical University in Prague, Faculty of Mechanical Engineering

Abstract: This thesis work was assigned by Czech Technical University in Prague, further CTU. It is a leading technical University in Czech Republic, located in the country capital, Prague. The purpose of this study is to investigate the stresses and displacements in human eye and instrument during endoscopic procedure. The results of the calculations will be used on developing the instrument for ophthalmic operations. In the process, the eye is penetrated by a needle-like endoscope to visually study the inner parts of the eye before or during the actual surgical operation. The need of further knowledge, especially in the behavior of the eye and the instrument, is still gathered. Because of fairly complicated nature of the interaction between viscoelastic human tissue and metallic material. Recommendations for future research on this field are made.

Keywords: ophthalmology, endoscopy, FEA, biomechanical engineering, optomechanics

1 Introduction

The story of ophthalmic applications of endoscopy can be dated time between the great world wars. In year 1934 procedure was first described by Dr. Harvey E. Thorpe, a native Latvian who immigrated to US in Pittsburgh in 1906. According to Pittsburgh Opthalmology Society [1], Thorpe received his bachelor degree from electrical engineering and did his post-graduate work in ophthalmology in New York City. As a true interdisciplinary, Thorpe designed an instrument which combines Galilean telescope and an illumination source. The whole instrument shaft (6.5 mm) [2] was inserted to eye thru 8 mm scleral incision.

Thorpe's design was revisited in 1978 with slight modifications by J.L Norris & G.W Cleasby. These two gentlemen, mentioned previously, improved [3] the original design with smaller rigid shaft (1.7 mm). In 1990, V,V Volkov et al. [4] introduced three types of flexible ophthalmo endoscopes which could be used directly to examine the interocular structures. Soon after the laser units where implemented to the endoscopes [5] and therefore, made possible to proceed surgical operations with the same instrument. From that point the prototypes had developed rapidly. All the components had been optimized and the image resolution had improved significantly [6].

Late in the autumn 2019 Dr. Hošek suggested me this topic because of my earlier knowledge and interest for finite element analysis. They had a problem with ophthalmic endoscope in developing. They wanted to improve the endoscope structure by making it more compact and provide better resolution image. During this process they faced a problem with the mechanical endurance of the optical part of the endoscope. Therefore, there was a need for study how much the critical parts can hold a load during the operation. This is done in order to optimize the design without having to compromise between the wanted qualities and strength.

2 Review of the study

Because of the fairly complicated mechanical system of mechanical tool which is interacting with organic tissues is the issue. This makes the study particularly interesting in a simulation point of view. Finite element method had been increasingly applied to biomechanical problems since late nineties. In twenty years the most successful biomechanical applications have been in the field of fracture mechanics of the human bones. These studies are done in the field of fracture mechanics. Mainly because of the solid material knowledge, the method has been successfully applied. These studies have helped researchers to understand the human bone fracture mechanism. On the contrary, the interaction of nonbiological and biomechanical structures has been studied far less. Main reason for this has been the limited computational power. Increasing computational capacity and improved algorithms allow us to study more and more complicated systems without sacrificing the accuracy to the simplifications.

For modeling the operational use of an ophthalmic endoscope, we are using the finite element method. It is a numerical method for solving partial differential equations in boundary value problems. In order to solve extremely complicated systems and the interactions between different bodies, this method subdivides a large system to a finite number of small elements. These elements are solved individually and they finally form a system of algebraic equations. The simple equations that model these finite elements are then assembled into a larger system that covers the entire problem.

The main target of this study is to study the stresses and displacements during ophthalmic surgery. The results of this study could be used for the development of the instrument for ophthalmic operations. The interest is, especially, in the optical part of the instrument and its capability to withstand external loading. The final output is to find the simplest model as possible with the highest possible accuracy.

2.1 Ophthalmic surgery

One of the main problems in this study is that it is controlled directly by the surgeon's hand and therefore the range of operational loading is wide and hard to define. During the ophthalmic operation, the surgeon needs to move the endoscope inside the eye in all directions. Even though the human eye is a very fragile organ and therefore requires extreme care during the surgical procedure, there might occur some forces high enough to damage the weakest parts of the instrument structure.

Although the ophthalmic endoscopes have been around for 1934. According to Marra, K et al, the popularization of ophthalmic endoscopy has been promoted by recent technological advancements that increased the number of indications for endoscopy [6]. Dr. Martina Nemčoková who is a doctor of Opthalmology from Charles University said that according to their experience the endoscopic examinations are mainly done for infants where, because of natural reasons, every move is done with high care [7]. Even though that the endoscopic view provides two fundamental advantages it is a relatively rarely used tool in ophthalmological operations. These advantages are: firstly, it reaches areas which are normally not so easy to examine because it passes anterior segment and it eases the visualization of anterior structures such as ciliary bodies and sub-iris space. Together these two advantages provide a steady base for surgery. From the following figure (1) we can see the scheme of ophthalmic operation with an endoscope.

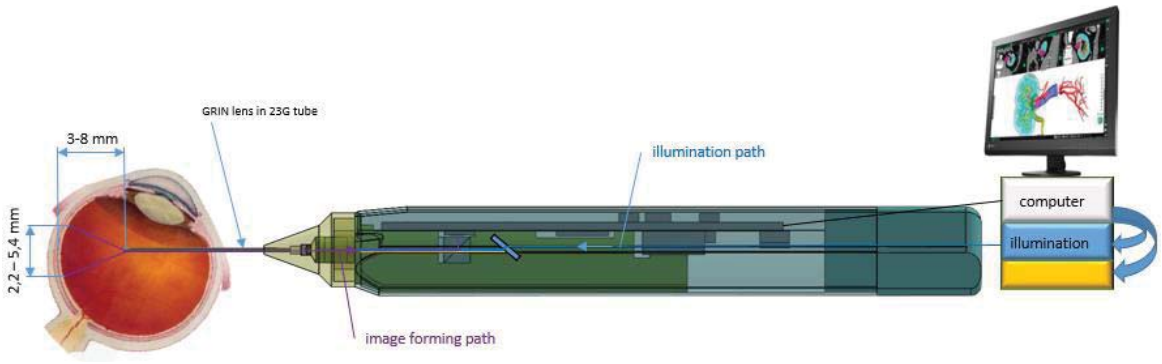

Figure 1. Schematic picture of endoscopic examination [8]. (Němcová. Š, Presentation. Modified)

2.2 Finite Element Model

In this study, we will create a model and we increase the model complexity in phases by increasing the number of non-linearities until we meet the measured values. We will compare the results between several models and subsequently our results will be compared between each other and with the results of similar cases, previously published in the literature. The model will be executed as a multibody model which means that part of the boundary conditions is in the interactions between the different bodies. The definition of these boundary connections will be found by iterative means. The most critical one is the interaction between the endoscope needle and the combined body of sclera, choroid, and retina. In this study, we are simplifying these previously mentioned parts into one and assume that they act as one unit under applied stress.

From the figure (2) we can see the CAD-model of the eye we are going to use in the analysis. From the table (1) we can see the mechanical properties of each body in the model.

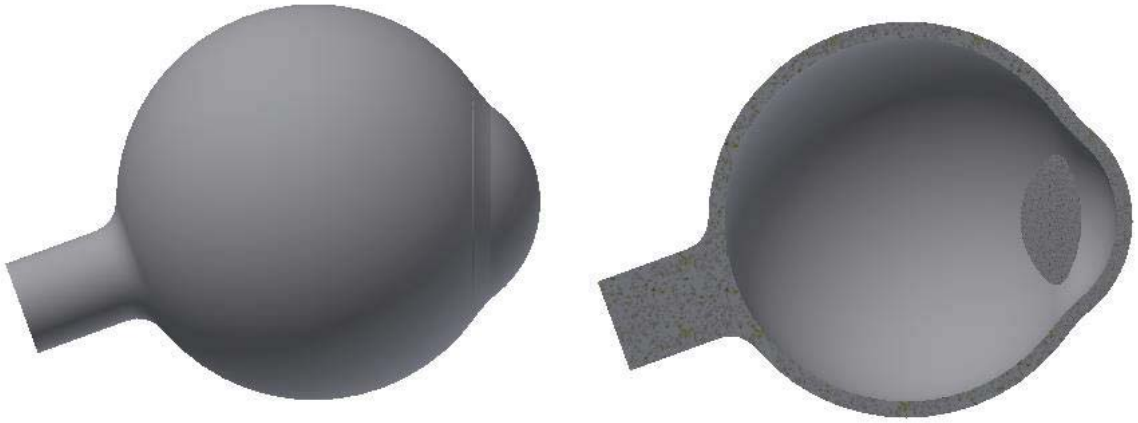

Figure 2. Eye model

Table 1. Mechanical properties of the eye model.

Tissue	E (Pa)	Poisson's ratio	C10 (Pa)	D1 (Pa^-1)	k (m/s)	Source(s)
Choroid	6,00E+05	0,49	100671,1	2,00E-07	5,00E-13	[9,10]
Cornea	2,90E+05	0,42	51056,34	3,31E-06	2,20E-11	[11,12,16]
Lens	8,20E+05	0,47	139455,8	4,40E-07	1,10E-12	[13,14]
Sclera	2,35E+06	0,47	399659,9	1,50E-07	6,37E-11	[9,12,18]
Aquenous humour	4,20E+04	0,49	7047	2,90E-06	1,00E-03	[15]
Vitreous humour	4,20E+04	0,49	7047	2,90E-06	1,00E-03	[15]

In the following figure (3) is named all the major parts of the human eye. Dimensions for annotations presented in the figure can be found in the table (2).

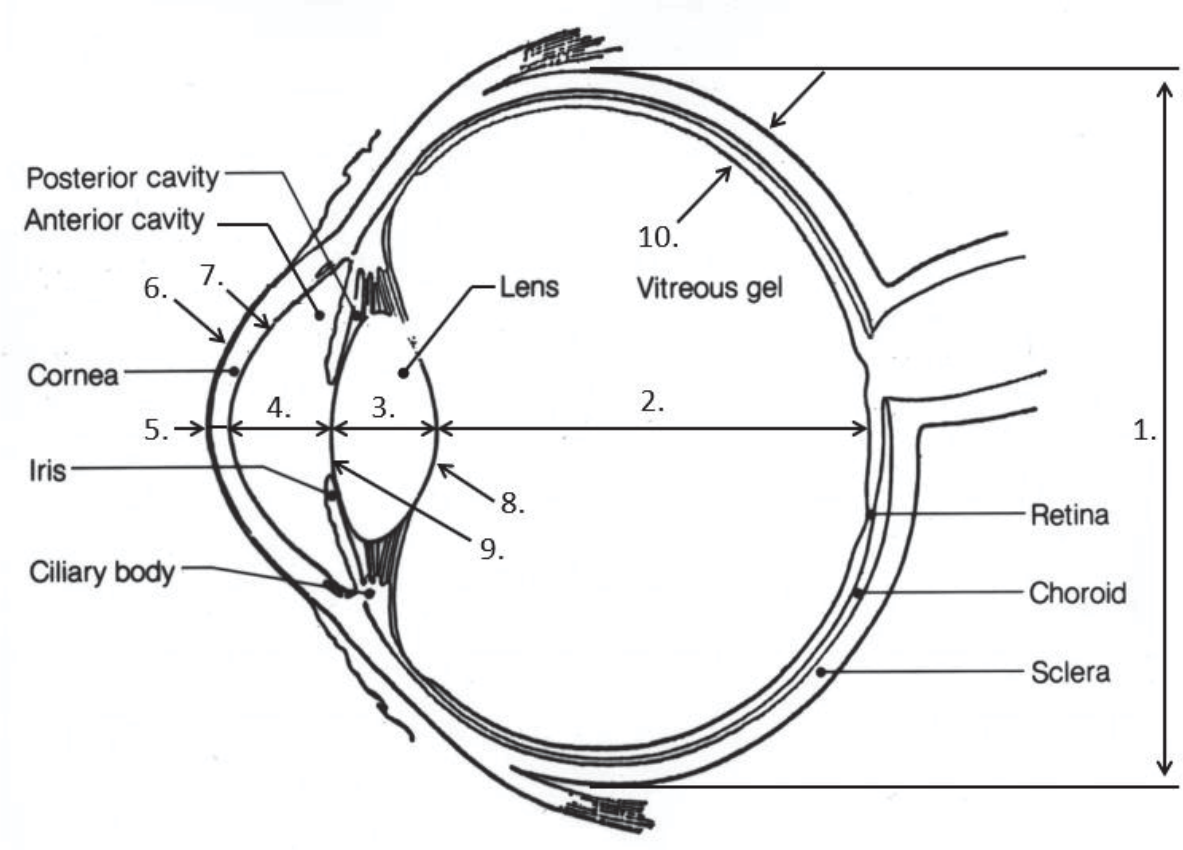

Figure 3. Main parts of human eye [19] (Clusters. E, home page, modified)

In the following table (2) we are presenting the characteristic dimensions of the eye. The CAD-model is based on the following values.

Table 2. Characteristic dimensions of human eye.

Annotation	Dimension	Unit	Source
1.	24	mm	[20]
2.	16	mm	[20]
3.	3,5	mm	[20]
4.	3,3	mm	[20]
5.	0,5	mm	[20]
6.	7,7	mm	[20]
7.	6,8	mm	[20]
8.	6	mm	[20]
9.	11	mm	[20]
10.	0,94	mm	[21]

In the table parameters C_{10} and D_1 are representing the neo-Hookean constants derived from the Young's modulus and Poisson's ratio data. Constant k represents the hydraulic permeability, which is a constant connected to the viscoelastic material model to capture the liquid flow in the porous material. Calculation method for constants C_{10} and D_1 are presented after next chapter.

Mooney-Rivlin models were introduced by Melvin Mooney in 1940 whom theorem was expressed in terms of invariants by Ronald Rivlin in 1948 [22,23]. It is important to realize that the Mooney-Rivlin model does not give any specific insight into the material behavior. Mooney-Rivlin is a curve fits of polynomial to test data. The numerical values of coefficients are results from the curve-fits. These coefficients are given to the FE analysis and they define how stiff the material is under the applied load. Hyperelastic models are defined thru a strain energy potential. Sometimes term strain energy function is used. strain energy potential is commonly denoted as (W) and it can be expressed as a function of the main strain invariants as following,

$$W = W(I_1, I_2, I_3). \tag{1}$$

Equation 1. Starin energy potential as a function of invariants [24]

If we assume that the material is isotropic then the I_3 term always equals 1. This is because when the $\varepsilon = 0$ the $\lambda = 1$. This is caused by the initial assumption of isotropic material. From following equation, we can see why the third invariant is one,

$$I_3 = \lambda_1^2 \cdot \lambda_2^2 \cdot \lambda_3^2 = \left(\frac{V}{V_0}\right)^2. \tag{2}$$

Equation 2. Third invariant [24]

In equation (3) the $\frac{V}{V_0}$ represents the volume ratio. The rest of the invariants are expressed as following (3 & 4),

$$I_1 = \lambda_1^2 + \lambda_2^2 + \lambda_3^2\,, \tag{3}$$

Equation 3. First invariant [24]

$$I_2 = \frac{1}{\lambda_1^2} \cdot \frac{1}{\lambda_2^2} \cdot \frac{1}{\lambda_3^2}\,. \tag{4}$$

Equation 4. Second invariant [24]

As we can see from the previous equations (2,3 & 4) the main invariants are defined by stretch ratios (λ) which are the ratios of initial lengths in the local principal directions (1, 2, 3). The stretch ratio can be expressed by the help of the relative strain, commonly known as an engineering strain.

$$\lambda = 1 + \varepsilon_{eng} \tag{5}$$

Equation 5. Strech ratio expressed with the help of engineering strain [25]

In the previous equation (6) the sub note (*eng*) indicates the engineering i.e. relative strain. The polynomial form is based on the first and second invariants and its general form can be seen in following,

$$W = \sum_{i+j}^{N} C_{ij} \cdot (I_1 - 3)^i \cdot (I_2 - 3)^j + \sum_{k=1}^{N} \frac{1}{D_1} \cdot (J_{el} - 1)^{2k} \tag{6}$$

Equation 6. Strain energy potential in a common form for two term Mooney-Rivlin. [24,25]

Even though the majority of the material models are to be taken from literature, we need to make some material testing to cover our assumptions. Because we are assuming combined bodies in the eye main structure we need to define the combined material properties. This can be done by using nanomechanical testing. This method is mainly used when defining elastic properties for biomaterials and soft tissues. The method is called quasistatic nanoindentation and it is usually used to define the common elastic properties like Young's modulus and Poisson's ratio. From those measured properties we can calculate the visco- and hyperelastic Mooney-Rivlin's two first constants and compare them to values previously published in related literature. The method of calculations is presented in the following formulas (1 & 2).

$$C_{10} = \frac{\mu}{2} \tag{7}$$

Equation 7. constant C_{10} first Mooney-Rivlin term [26]

$$D_1 = \frac{\lambda}{2} \tag{8}$$

Equation 8. constant D_1 Second Mooney-Rivlin term [26]

Where λ and μ are called Lamé coefficients. They can be derived from bulk modulus by using following formula.

$$B = \lambda + \frac{2}{3} \cdot \mu \tag{9}$$

Equation 9. Bulk modulus writed in terms of Lamé first and second coefficent [26].

Where B can be written in a terms of Young's modulus and Poisson's ratio as following.

$$B = \frac{E}{3(1 - 2 \cdot \nu)} \tag{10}$$

Equation 10. Bulk modulus written as a function of Young's modulus and Poisson's ratio [26].

Also Lamé's first parameter can be re-written by Young's modulus and Poisson's ratio.

$$\lambda = \frac{E \cdot \nu}{(1 + \nu) \cdot (1 - 2 \cdot \nu)} \tag{11}$$

Equation 11. Lamé's first parameter written as a function of Young's Modulus and Poisson's ratio [26].

By using these previous formulas we can solve the Lamé's second parameter as following,

$$\Longrightarrow \mu = \frac{3 \cdot (B - \lambda)}{2}. \tag{12}$$

3 Future development

In the future, we will proceed with the simulation of the endoscope-eye interaction. We are expecting to found that defining the interactions of the different bodies is fairly complicated and time-consuming. There are not much-verified results of similar cases available and therefore we need to rely on specialist dictums and our own perceptions when it comes to determining that boundary conditions are working correctly. The usage of the PHE (porohyperelastic) material model is still a discretionary option. We are expecting to found sufficiently accurate results by using the standard neo-Hookean constitutive approach in material models. For model verification, we are going to use pigs eye. According to Dr. Nemčoková, this is structurally really close to the human eye. According to her, pig eyes are widely used in University teaching when the purpose is to mimic the human eye therefore it shall be suitable in this application too. Model verification will be done by comparing the measured deformation to simulate one.

Acknowledgement
This work was supported by the Grant Agency of the Czech Technical University in Prague, grant No. SGS20/055/OHK2/1T/12.

References

[1] *Harvey E. Thorpe, MD*: P.O.Socienty 2019. Jan 2020. Available: www.pghoph.org.
[2] Thorpe H. *Ocular endoscope: instrument for removal of intravitreous nonmagnetic foreign bodies*. Trans Am Acad Ophthalmol Otolaryngol. 1934; 39, pp. 422–424
[3] Norris J. L & Cleasby G.,W. *An endoscope for ophthalmology*. Am J Ophthalmol. 1978; 85, pp.420–422
[4] Volkov V.V, Danilov AV, Vassin LN, Frolov YA. *Flexible endoscope for intraocular surgery*. Arch Ophthalmol. 1990; 108 pp. 1037–1038.
[5] Uram M. *Ophthalmic laser microendoscope endophotocoagulation*. Ophthalmology. 1992; 99, pp. 1829–1832.
[6] Marra K. V., Yonekawa, Y., Papakostas, T. D., & Arroyo, J. G. (2013). *Indications and techniques of endoscope assisted vitrectomy*. Journal of ophthalmic & vision research, 8(3), pp. 282–290.
[7] Nemčoková M. MD, *Ophthalmological surgery*. 2020. Interview on 24.1.2020. Interviewer Mastomäki, J. Prague
[8] Němcová Š. Ing. PhD. 2019. CTU in Prague. Faculty of Mechanical Engineering. Presentation. Requires access right.
[9] Friberg T.R, Lace J.W. *A comparison of the elastic properties of human choroid and sclera*. Exp Eye Res. 1988; 47, pp. 429–436.
[10] Woo S.L, Kobayashi A.S, Schlegel WA, Lawrence C. *Nonlinear material properties of intact cornea and sclera*. Exp Eye Res. 1972; 14, pp. 29–39.
[11] Hamilton K.E & Pye D.C. *Young's modulus in normal corneas and the effect on applanation tonometry*. Optom Vis Sci. 2008; 85 pp.445–450.
[12] Uchio E, Ohno S, Kudoh J, Aoki K & Kisilewicz L.T. *Simulation model of an eyeball based on finite element analysis on a supercomputer.* Clinical Science. 1999; 83 pp. 1106–1111.
[13] Fisher R.F. *Elastic constants of the human lens capsule*. J Physiology. 1969; 201, pp. 1–19
[14] Fisher R.F & Wakely J. *The elastic constants and ultrastructural organization of a basement membrane (lens capsule)*. Proc R Soc Lond B Biol Sci. 1976; 193, pp 335–358.
[15] Cirovic S, Bhola R.M, Hose D.R, Howard I.C, Lawford P.W & Parsons M.A. *A computational study of the optic nerve evulsion. IUTAM Preoceedings on Impact Biomechanics*: From Fundamental Insights to Applications. 2005, pp. 469–476.
[16] Overby D, Ruberti J, Gong H, Freddo T.F & Johnson M. *Specific hydraulic conductivity of corneal stroma as seen by quickfreeze/ deep-etch*. J Biomech Eng. 2001; 123 pp. 154–161.
[17] Johnson M & Erickson K. *Mechanisms and routes of aqueous humor drainage.*
[18] Jackson T.L, Hussain A & Hodgetts A. *Human sclera hydraulic conductivity: age-related changes, topographical variation,and potential scleral outflow facility*. Invest Ophthalmol. 2006, 47, pp. 4942–4946.
[19] Custers E. 2017 *Anatomy of the Eye: Human Eye Anatomy.* Jan 2020 Available: www.owlcation.com/stem/Anatomy-of-the- Eye-Human-Anatomy.
[20] Atchison, David A. and George Smith. 2000. *Optics of the Human Eye.* 1.th ed. Oxford: Butterworth-Heinemann.
[21] Vurgese, S., Panda-Jonas, S., & Jonas, J. B. 2012, Jan 2020 *Scleral thickness in human eyes*. PloS one, 7(1), Available: https://doi.org/10.1371/journal.pone.0029692
[22] Mooney, M., 1940, *A theory of large elastic deformation*, Journal of Applied Physics, 11 (9), pp. 582–592.
[23] Rivlin, R. S., 1948, *Large elastic deformations of isotropic materials*. *Further developments of the general theory*, Philosophical Transactions of the Royal Society of London. Series A, Mathematical and Physical Sciences, 241(835), pp. 379–397.
[24] Ansys, Inc. 2005, *Hyperelastic Materials,* Handbook. Jan 2020 Available: http://read.pudn.com/download222/doc/1047742/modelling_simulation/nonlinear-materials-tech+++.pdf
[25] McGinty, B. 2012. Homepage. *Mooney-Rivlin Models*. Jan 2020, Available: https://www.continuummechanics.org/mooneyrivlin.html
[26] Pence T & Gou K. 2014. *On compressible versions of the incompressible neo-Hookean material.* Mathematics and Mechanics of Solids. Available: https://doi.org/10.1177%2F1081286514544258

Selected article from
Tento dokument byl publikován ve sborníku

Nové metody a postupy v oblasti přístrojové techniky, automatického řízení a informatiky 2020

New Methods and Practices in the Instrumentation, Automatic Control and Informatics 2020

14. 9. – 16. 9. 2020, Zámek Lobeč

ISBN 978-80-01-06776-5

Web page of the original document:
http://iat.fs.cvut.cz/nmp/2020.pdf

Obsah čísla/individual articles:
http://iat.fs.cvut.cz/nmp/2020/

Ústav přístrojové a řídicí techniky, FS ČVUT v Praze, Technická 4, Praha 6